

Alloy scattering of substitutional carbon in silicon: a first principles approach

M.P. Vaughan¹, F. Murphy-Armando¹ and S. Fahy^{1,2}

¹Tyndall National Institute, Lee Maltings, Cork, Ireland;

²Department of Physics, University College Cork, Ireland

1. Abstract

A method is developed to obtain the alloy scattering coefficients from first-principles band structure calculations. It is found that the scattering matrix can be decomposed into two additive components: a chemical part due to atomic substitution and a part due to ionic relaxation. The method is then applied to find the intra- and inter-valley electron scattering rates for substitutional carbon in silicon. Intravalley scattering is found to be the dominant process.

2. Introduction

The introduction of carbon into SiGe/Ge heterostructures is of technological interest due the dual effects of strain-compensation in the $\text{Si}_{1-y}\text{Ge}_y$ layers [1] and suppression of the out-diffusion of p -type acceptors, in particular boron [2] and indium [3], during wafer fabrication. The transport properties of the material are then expected to be modified by two competing processes. On the one hand, in silicon, the induced strain will lift the degeneracy of the Δ valleys allowing the conduction electrons to see a smaller effective mass. On the other hand, the substitutional carbon is likely to introduce alloy scattering, acting to reduce the mobility.

A method is developed to obtain the alloy scattering matrix from density functional theory (DFT) calculations based on a similar approach successfully used to investigate scattering in SiGe alloys [4, 5]. It is found that the scattering matrix can be decomposed into two additive components: a chemical part due to the substitution of a Si atom by a C atom and a part due to the relaxation of Si atoms around the C substitutional site that we have modeled in terms of the phonon deformation potential. The method is then applied to find the intravalley and intervalley electron scattering matrix for substitutional carbon in silicon. It is found that intravalley scattering is the dominant process. However, we find that alloy scattering due to substitutional carbon is too weak to reduce the mobility to the degree observed in strained $\text{Si}_{1-x}\text{C}_x$ layers [6] and therefore support the conclusion that this degradation is due to charged interstitial carbon complexes.

3. Alloy scattering

The generally accepted parametric model of alloy scattering in semiconductors is that due to Harrison and Hauser [7], based on the formalism of random potential fluctuations against an average potential (the virtual crystal approximation (VCA) [8]) Harrison and Hauser considered only completely random alloys and employed the scattering model of a spherical square well potential extending no further than the primitive cell. Moreover, the scattering potential in the Harrison-Hauser model is not directly related to the electronic structure of the alloy and most modelers still treat this potential as a fitting parameter.

In an investigation of the actual physics involved in alloy scattering, Murphy-Armando and Fahy [4] pursued a first principles approach, in which the alloy scattering parameters were obtained directly from matrix elements between band states of the change in potential, ΔV , which is caused by substituting one atom type with the other type at a given lattice site. These matrix elements are calculated in a supercell geometry, where the substitutional lattice site is placed in a large but finite cell with periodic boundary conditions. The supercell geometry allows standard DFT methods to be applied to the calculation of the single-particle potential and the structural relaxations around the substitutional site. Scattering matrix elements $\langle n, \mathbf{k} | \Delta V | n', \mathbf{k}' \rangle$ can be found for those wavevectors \mathbf{k} and \mathbf{k}' that differ by a reciprocal lattice vector of the supercell ($\mathbf{k}' = \mathbf{k} + \mathbf{G}_{SC}$). The single electron eigenvalues and wave functions of states required to construct the matrix elements are calculated from the ground-state charge density obtained from self-consistent DFT calculations. The formalism of this approach naturally incorporates potentials extending beyond the primitive cell, including the effects of both pseudopotential difference and ionic relaxation. The arbitrariness of choosing a scattering potential model is therefore removed and the physical effects of different ionic species may be isolated from those of ionic relaxation.

The first principles approach developed in the current work differs in its formalism from that of the previous methods [4-5]. In those earlier papers, the scattering

matrix elements for intervalley and intravalley scattering were obtained from a reduced matrix that involved only single-particle states that were periodic in the supercell, corresponding to scattering between Bloch states $|n, \mathbf{k}\rangle$ with wave vector $\mathbf{k} = \mathbf{G}_{SC}$, a reciprocal lattice vector of the supercell Bravais lattice. A problem with this method arises in the case of intravalley scattering ($\mathbf{k} \approx \mathbf{k}'$) since the calculation of the matrix element involves the difference between the eigenvalues of the systems with and without a substituting ion. However, the pseudopotentials of the ionic species are only determined to an arbitrary constant in a periodic lattice. A common reference energy may then only be inferred by some scheme of matching the supercell potentials far from the substitutional impurity.

In the present work, an alternative approach is used based on scattering between states that are not periodic in the supercell and for which $\mathbf{q} = \mathbf{k} - \mathbf{k}' = \mathbf{G}_{SC} \neq 0$. The intravalley scattering is then found by interpolating the scattering matrix elements $\langle n, \mathbf{k} | \Delta V | n', \mathbf{k}' \rangle$ to $\mathbf{q} = 0$. This yields a model that does not rely the absolute difference between the perturbed and unperturbed energy eigenvalues, thereby circumventing the need to find a common reference energy in the calculation of the intravalley scattering.

4. Overview of the method

The method of obtaining the alloy scattering parameters described here is based on first principles DFT calculations for Si supercells with a single carbon impurity. The introduction of an impurity leads to a coupling of Bloch states at points \mathbf{k} and \mathbf{k}' of the Brillouin zone, for which $\mathbf{q} = \mathbf{k} - \mathbf{k}' = \mathbf{G}_{SC}$, a reciprocal lattice vector of the supercell. As the size of the supercell is increased in real space, its reciprocal lattice includes shorter (non-zero) vectors \mathbf{G}_{SC} . Our task is to extract the matrix elements of this scattering matrix from the eigenvalues and eigenstates of the self-consistent field calculations (SCF) obtained via DFT. To this end, we construct large supercells with a single carbon impurity and perform calculations with (a) no relaxation and (b) relaxation of the ionic positions.

5. Ionic relaxation

Ionic relaxation has a significant effect on the scattering matrix. In the course of the present investigations we have found that the scattering matrices with ionic relaxation depend not only on the magnitude of the scattering wavevector but also on the direction. Our investigations indicate that the scattering matrix may be decomposed into two additive contributions: one due to the chemical change upon atomic substitution and the other due to the relaxation of the atoms surrounding the substitutional site.

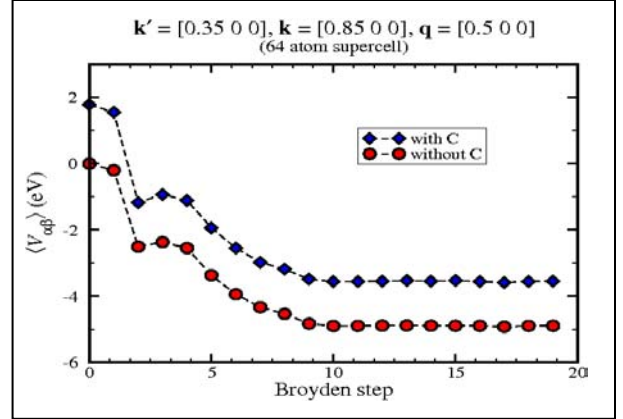


Fig.1: The scattering matrices calculated at each Broyden step in the ionic relaxation algorithm for Si(63)C(1) (diamonds) and Si(64) (circles) with the same ionic positions. Here the scattering is for $\mathbf{q} = (2\pi/a_0)[1/2 \ 0 \ 0]$ (parallel to the Δ line) from the Δ valley minimum.

When a defect atom substitutes in a periodic lattice, the surrounding atomic positions relax. This relaxation may be found using density functional theory, where we use the Broyden-Fletcher-Goldfarb-Shanno relaxation algorithm [9-11] to vary the positions of the atoms in the supercell until the atomic forces are all zero. This gives the relaxed positions of the atoms in the presence of the C substitutional defect. We have investigated the effect of atomic relaxation on the scattering matrix element as follows: we have taken the atomic positions generated in the various steps of the relaxation algorithm (we call these ‘Broyden steps’) in finding the equilibrium structure surrounding the defect atom and we have calculated the carrier scattering matrix element with (a) a C atom and (b) a Si atom at the central site for each arrangement of surrounding atoms..

An example of the results is shown in Fig 1 for scattering from the Δ valley minimum parallel Δ line. The similarity between the structures with and without the carbon is quite striking, the variation with Broyden step closely matching for the two structures. The graph shown is representative of this behaviour that was repeated for all other scattering vectors calculated. Thus, we see that the displacement of the Si atoms, relaxing around the C impurity, makes the same contribution to the scattering matrix element in a pure Si crystal as it does with the C atom present.

In order to gain insight into the physics, we have developed a model based on the deformation potential. The scattering matrix derived bears a close resemblance to the coupling coefficient for acoustic phonon scattering and maybe interpreted as scattering from a superposition of frozen phonons.

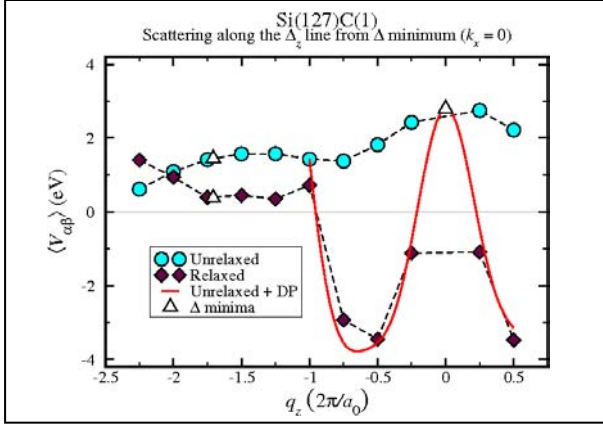


Fig.2: Matrix elements for scattering along the Δ line. The circles are for scattering in the unrelaxed structure, the diamonds for the relaxed supercell. The clear triangles are obtained from polynomial interpolations of the data at $\mathbf{q} = 0$ (on the right) and g -type scattering from one Δ valley minimum to the other (on the left). The solid line is obtained by adding the matrix element for deformation potential scattering model to the interpolating polynomial of the unrelaxed structure. We note that this is very close to the results for scattering in the relaxed structure over the region corresponding to intravalley scattering.

5. Results

Figure 2 shows the matrix elements for scattering along the Δ line from the Δ valley minimum, indicated in the graph as $\mathbf{q} = 0$. The six points on the right-hand-side of Fig. 2 correspond to points in the $+k_z$ half of the primitive BZ and are those for intravalley scattering. The points on the left-hand-side of the graph are for g -type intervalley scattering from the Δ valley minimum along the $+k_z$ axis. The light circles are for the unrelaxed structure and, as can be seen, vary quite smoothly. Hence we have confidence in interpolating these points to $\mathbf{q} = 0$, yielding a value of 2.806 ± 0.004 eV (shown on the graph as a clear triangle). The dark diamonds are the matrix elements for the relaxed structure, which show a much sharper variation. However, we find that when we add the polynomial fit for the unrelaxed structure to the matrix element calculated from our model based on the deformation potential (solid line on the graph), the curve follows the relaxed scattering matrix elements very well. Note that no fitting of this curve to the relaxed points has been used. In this case, the deformation potential tensor elements for silicon were calculated using a frozen phonon approach [5], which gave values of $\Xi_d = -0.029$ eV and $\Xi_u = 8.77$ eV. Note that the value of Ξ_d has not been obtained to the same degree of confidence as Ξ_u .

Since the deformation potential model predicts zero scattering for $\mathbf{q} = 0$, we take the matrix element for the relaxed structure at $\mathbf{q} = 0$ to be equal to that of the unrelaxed structure.

The results for g -type intervalley scattering, in which the scattering is into the valley diametrically opposite the initial valley along the same Cartesian direction, are shown on the left hand side of Fig 2. Here the results for the both the unrelaxed and relaxed structures are smooth and we are easily able to interpolate to $\mathbf{q} = -1.7$ (in reduced coordinates) corresponding to scattering from one Δ valley minimum to the other diametrically opposite it. The values found are 1.44 ± 0.03 eV for the unrelaxed supercell and 0.35 ± 0.05 eV for the relaxed supercell.

The results for f -type scattering intervalley scattering (not shown), in which the scattering is from a valley lying along one Δ line to one of the other four valleys lying in an orthogonal direction, are -1.4 ± 0.05 eV for the unrelaxed structure and 0.1 ± 0.15 eV for the relaxed.

Using the results for the relaxed structures, the alloy scattering-limited mobility has been calculated and compared to the experimental results of Eberl *et al* [12] and Osten *et al* [6]. The results are shown in Fig. 3. Both groups of researchers find the same mobility for unstrained Si (shown as clear circles and clear triangles). For 0.4% carbon, Eberl *et al* find an increase in the mobility, particularly at low temperature where the enhancement due to the lifting of the Δ valley degeneracy is greatest. The $0.5 \mu\text{m}$ thick $\text{Si}_{1-x}\text{C}_x$ and Si reference layers were phosphorous doped with the same nominal concentration of about $3 \times 10^{17} \text{ cm}^{-3}$. The calculated alloy scattering-limited mobility for this concentration is shown in comparison (solid line). Apart from the low temperature peak, the calculated mobility is consistent with the experimental results, showing that the alloy scattering due to substitutional carbon may contribute to the resistivity but is not the limiting process.

The work of Osten *et al*, on the other hand, shows a degradation of the mobility, even for lower C concentrations. These researchers grew $0.2 \mu\text{m}$ thick $\text{Si}_{1-x}\text{C}_x$ layers with a nominal antimony doping of 10^{17} cm^{-3} . Shown on the graph are their results for 0.31% (filled circles) and 0.57% (filled squares), between which we might expect Eberl *et al*'s results to lie. Note that as well as the suppression of the mobility at higher temperatures following a $T^{-1/2}$ dependence, consistent with alloy scattering, there appears to be additional limiting processes at lower temperatures following a $T^{3/2}$ dependency, characteristic of ionised impurity scattering. Indeed, Osten *et al* argue for the formation of electrically active defects due interstitial carbon complexes suppressing the mobility. The results of the present work for $x = 0.31\%$, shown on the graph as the dashed line are consistent with this argument in that the scattering due to substitutional carbon is too weak to limit the mobility to the degree found.

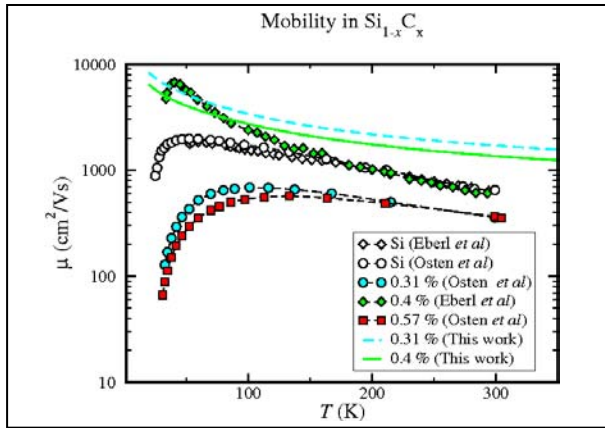


Fig.3: Experimental mobilities for strained $\text{Si}_{1-x}\text{C}_x$ and the calculated alloy scattering-limited mobilities. The mobility for unstrained Si is shown as clear circles and clear triangles. For 0.4% C, the work of Eberl *et al* (filled diamonds) shows an increase in the mobility. The calculated alloy scattering-limited mobility for this concentration is shown in comparison (solid line). The work of Osten *et al* shows a degradation of the mobility, even for lower C concentrations. Here we show their results for 0.31% (filled circles) and 0.57% (filled squares). For comparison, the calculated alloy scattering-limited mobility for 0.31% is also shown (dashed line).

4. Conclusions

In the present work, a method of obtaining the alloy scattering matrix elements from density functional theory calculations has been developed. This is consistent with the existing formal model of alloy scattering and the matrix elements can be obtained from a perturbation in a large supercell without having to restrict the perturbing potential to the direct space primitive cell. More importantly, the approach taken here seeks the physical origin of the alloy scattering potential that heretofore has been unknown and is usually varied in mobility calculations as a fitting parameter. The development of the approach described here allows us to circumvent the problem of the arbitrary zero of the pseudopotentials, allowing us to obtain results for intravalley scattering more reliably.

Additionally, we have found strong evidence that the scattering matrix can be decomposed into two additive contributions: (a) a chemical contribution, arising from substitution of different chemical species (or in our case, pseudopotentials) and (b) a contribution due to ionic relaxation. A simple model of the latter in terms of the deformation potential has been developed that accounts well for intravalley scattering perpendicular to the Δ line.

The application to $\text{Si}_{1-x}\text{C}_x$ has shown that intravalley scattering is the dominant alloy scattering process, with a matrix element of 2.81 eV and that f -type and g -type scattering are negligible in comparison (-1.1 eV and 0.35 eV respectively). However, the calculated alloy scattering-limited mobility for non-degenerate bands

shows that the alloy scattering due to substitutional carbon is too weak to produce the reduction in mobility observed by Osten *et al* [6]. This supports the conclusions of these researchers that the mobility degradation in their $\text{Si}_{1-x}\text{C}_x$ samples is due to interstitial carbon complexes.

This work was supported by the Science Foundation Ireland.

References

- [1] S.C. Jain, H.J. Osten, B. Dietrich and H. Rücker, *Semicond. Sci. Tech.* **10**, 1289 (1995)
- [2] H.J. Osten, H. Rücker, J.P. Liu and B. Heinemann, *Microelectron. Eng.* **56**, 209 (2001)
- [3] C.F. Tan, E.F. Chor, J. Liu, H. Lee, E. Quek and L. Chan, *Appl. Phys. Lett.* **83**, 4169 (2003)
- [4] F. Murphy-Armando and S. Fahy, *Phys. Rev. Lett.* **97**, 96606 (2006)
- [5] F. Murphy-Armando and S. Fahy, *Phys. Rev. B* **78**, 35202 (2008)
- [6] H.J. Osten and P. Gaworzewski, *J. Appl. Phys.* **82**, 4977 (1997)
- [7] J.W. Harrison and J.R. Hauser, *Phys. Rev. B* **13**, 5347 (1976)
- [8] L. Nordheim, *Ann. Phys* **9**, 607 (1931)
- [9] C.G. Broyden, *Math. Comput.* **21**, 368 (1967)
- [10] D. Goldfarb, *Math. Comput.* **24**, 23 (1970)
- [11] D.F. Shanno, *Math. Comput.* **24**, 647 (1970)
- [12] K. Eberl, K. Brunner and W. Winter, *Thin Solid Films* **294**, 98 (1997)